International Journal of Energy
ISSN: 2957-9473 | Vol. 9, No. 1, 2026

Mechanical Properties and Energy Evolution Law of Coal-Based Solid Waste Backfill at Different Temperatures and Ages

Longqiang Wei [1, 2, *], Zhiqiang Wen [2]

[1] Joint National-Local Engineering Research Centre for Safe and Precise Coal Mining, Anhui University of Science and Technology, Huainan, Anhui, 232001, China
[2] School of Mining Engineering, Anhui University of Science and Technology, Huainan, Anhui, 232001, China
*** Corresponding author:** Longqiang Wei

Abstract: The increasing use of deep coal mine backfilling operations under high geothermal conditions has drawn attention, The growing application of deep coal mine backfilling under elevated geothermal conditions has attracted increasing attention; however, the role of curing temperature in governing the mechanical response and energy evolution of coal-based solid waste backfill has not yet been fully clarified. In this study, coal gangue, fly ash, and desulfurization gypsum were selected as representative coal-based solid waste constituents to systematically examine the mechanical behavior and energy evolution of cemented backfill subjected to different curing temperatures (20, 27.5, 35, 42.5, and 50 °C) and curing durations (3, 7, 14, and 28 d). Material characteristics were characterized using X-ray diffraction (XRD), scanning electron microscopy (SEM), and particle size distribution analysis. Displacement-controlled uniaxial compression tests were conducted to obtain stress–strain responses, while elastic strain energy and dissipated energy were quantified and analyzed on the basis of the first law of thermodynamics. The findings highlight that curing temperature has a marked age-dependent effect on the mechanical behavior of the backfill. At early ages (3, 7, and 14 days), increasing the curing temperature enhances the elastic modulus, peak stress, and peak strain. At 28 days, both strength and deformation capacity reach their maximum values at 42.5 °C, whereas increasing the temperature to 50 °C causes post-peak softening and a reduction in load-bearing capacity. Energy analysis reveals that, at 28 days, both elastic strain energy and total energy at the peak stress first rise and then decline as curing temperature increases, reaching maximum values of 35.92 kJ/m³ and 56.45 kJ/m³, respectively, at 42.5 °C. The energy evolution process can be categorized into four distinct stages: pore compaction, linear elastic deformation, yielding damage, and post-peak failure. Higher curing temperatures significantly increase the proportion of energy dissipated in the compaction stage (from 37.5% to 59.3%) while reducing the energy dissipated in the elastic stage, which accelerates the damage process under high-temperature curing.

Keywords: Curing Temperature; Coal-based Solid Waste; Energy Evolution.

1. Introduction

With the continuous advancement of green mining concepts, backfill mining has emerged as a core technique within modern green mining systems [1]. This method effectively alleviates problems such as coal resource loss beneath buildings, railways, and water bodies, while simultaneously reducing surface subsidence and facilitating the reutilization of coal gangue, fly ash, and other industrial solid wastes, thereby supporting sustainable coal resource development [2]. As mining activities progressively extend to greater depths, underground environments are increasingly subjected to elevated geothermal conditions. Pronounced regional variability in geothermal distribution and temperature gradients, arising from climatic and geological differences, leads to higher surrounding rock temperatures with increasing depth, which poses substantial challenges to the mechanical performance of backfill materials operating under complex thermal conditions.

Early research on the temperature-dependent behavior of cemented materials primarily concentrated on conventional geomaterials, including concrete [3,4]. In contrast, the thermal environment encountered by cemented backfill in underground mining is highly variable, owing to temporal evolution and site-specific geological conditions, resulting in intricate and dynamic thermal regimes. In recent years, numerous studies have systematically examined the influence of curing temperature on the mechanical behavior of cemented backfill. Nevertheless, due to disparities in temperature ranges, material compositions, and experimental methodologies, the reported conclusions remain partially inconsistent. Existing investigations generally indicate that curing temperature plays a decisive role in governing the mechanical performance of cemented backfill. Su Hongyan [5] identified the presence of a critical curing temperature, beyond which accelerated evaporation of free water inhibits hydration reactions, leading to reduced hydration products and increased pore development. Through multiscale thermo–mechanical coupling analyses, Li Zhi [6] demonstrated that elevated curing temperatures adversely affect the long-term strength evolution of cemented backfill. Chen Qiusong [7] reported that although early-age strength exhibits an exponential dependence on curing temperature, the compressive strength at later curing stages shows limited sensitivity to temperature variation. Moreover, a number of studies [8] have consistently shown that higher curing temperatures significantly enhance early hydration and strength development, whereas their influence on later-age strength may become marginal or even inhibitory. Considerable attention has also been directed toward elucidating the mechanical behavior and damage evolution mechanisms of cemented backfill under extreme thermal

conditions. Based on triaxial unloading tests, Liu Weizhen [9] observed that detrimental thermal stresses induced by high-temperature curing promote microcrack initiation during the post-peak stage, resulting in abrupt degradation and even reverse evolution of deformation modulus during confining pressure unloading. Bai Liwei [10] further investigated the acoustic emission characteristics of cemented backfill specimens cured at different temperatures and demonstrated that elevated temperatures suppress hydration reactions to a certain extent.

Fall et al. [12] conducted a systematic investigation into the temperature-dependent mechanical response and microstructural evolution of cemented backfill. Wu et al. [13] established predictive mathematical models to describe creep behavior of cemented backfill under varying thermal conditions. Based on three-point bending experiments, Wu Wenbin [14] investigated the fracture-related mechanical behavior of cemented backfill specimens cured under different temperature conditions. With particular attention to alpine environments, Liu Chao [15] assessed the mechanical performance of backfill materials, whereas Jiang Haiqiang [16] demonstrated that lower consolidation temperatures exert a significant influence on both compressive strength and stress–strain responses of cemented backfill. To examine the combined effects of multiple governing factors, Shi Lizhuang [17] conducted triaxial compression tests to evaluate the coupled impacts of curing age, thermal conditions, and confining pressure on the strength and creep characteristics of full-tailings cemented backfill. Yang Xiaoliang [18] employed fractal analysis and morphological characterization of shear fracture surfaces to elucidate the role of curing temperature in controlling the failure mechanisms of cemented backfill as well as its interface behavior with surrounding rock. Liu et al. [19] explored the effects of thermal conditions on the physical and microstructural properties of cemented backfill, indicating that excessively high curing temperatures lead to varying extents of mechanical degradation and microstructural damage. In a similar context, Duan Yun [20] reported that elevated steam-curing temperatures combined with extended curing durations negatively affect the later-age compressive strength of manufactured sand concrete.

Based on both domestic and international research efforts, substantial progress has been made in characterizing the mechanical behavior and strength development of cemented backfill through extensive experimental and theoretical studies. Nevertheless, investigations addressing curing temperature effects remain relatively limited, as existing research has predominantly focused on tailings backfill in metal mining, with insufficient attention devoted to applications in coal mine backfilling. Considering that backfill materials employed in coal mining are largely derived from coal-based solid wastes generated during coal extraction and utilization, it is therefore necessary to systematically examine the evolution of mechanical performance of coal-based solid waste backfill under different curing temperature regimes.

2. Test Materials and Schemes

2.1. Material Analysis

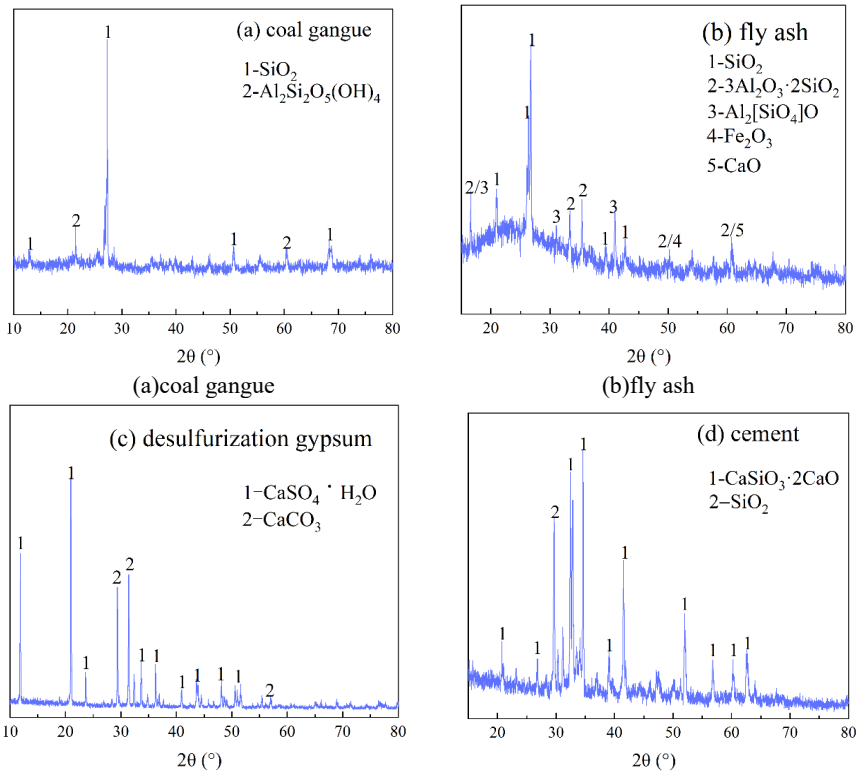


Fig 1. Material XRD analysis

In this study, the mineralogical compositions of coal-based solid waste backfill materials were characterized using X-ray diffraction (XRD). The mineral phases of three types of coal-based solid wastes and cement were systematically analyzed, and their particle size distributions were determined using a laser particle size analyzer. In addition, scanning electron microscopy (SEM) was employed to observe the microstructural morphology, thereby providing a

comprehensive understanding of the fundamental physical characteristics of the three coal-based solid wastes and cement.

(1)XRD analysis of experimental materials

The XRD patterns of the tested materials are shown in Fig. 1. As can be observed, the main diffraction peaks of coal gangue are concentrated in the range of 20°~30°, indicating that its primary mineral components are SiO_2 and Al_2O_3. The diffraction peaks of fly ash are also mainly distributed between 20° and 30°, with the dominant mineral phases identified as $3Al_2O_3 \cdot 2SiO_2$ and SiO_2. According to the XRD pattern of desulfurization gypsum, its major mineral constituents are $CaSO_4 \cdot 2H_2O$, accompanied by a small amount of $CaCO_3$. The XRD analysis of cement reveals that its primary components consist mainly of $CaSiO_3 \cdot 2CaO$ compounds, along with a minor presence of SiO_2.

(2) Material particle size analysis

Coal gangue with particle sizes ranging from 0 to 5 mm was selected as the aggregate material for the experiments. As illustrated in Fig. 2(a), the fly ash consists predominantly of fine particles, with the majority having sizes below 200 μm, and particles within the 15-95 μm interval accounting for the largest proportion. Fig. 2(b) shows that the particle size distribution of desulfurization gypsum is largely confined to the range of 15-95 μm. As depicted in Fig. 2(c), cement particles are mainly distributed between 15 and 60 μm, reflecting an overall fine particle size characteristic.

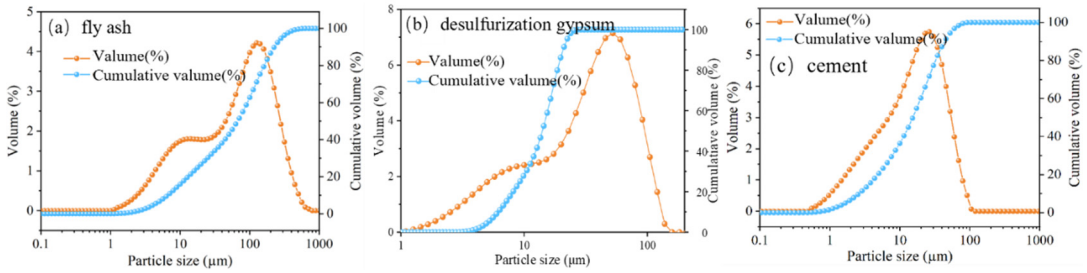


Fig 2. Material particle size analysis

(3)Material particle size analysis

As shown in Fig. 3(a), the coal gangue aggregates with a particle size distribution of 0-5 mm exhibits predominantly irregular block-like particles at the microscale, with rough surface features. The SEM image of fly ash in Fig. 3(b) reveals that spherical particles of various sizes dominate the microstructure, characterized by well-defined outlines and relatively smooth surfaces. As illustrated in Fig. 3(c), desulfurization gypsum presents an irregular blocky microstructure, with moderately sized particles that are relatively uniformly distributed. Figure 3(d) shows the SEM image of cement, in which the particles are primarily fine and irregular in shape. The relatively small particle size facilitates the diffusion of $Ca(OH)_2$ through the pore spaces within the mixture during hydration, allowing it to react with other constituents to form crystalline hydration products, such as ettringite. These hydration products progressively occupy the internal voids within the mixture, thereby improving the overall strength of the specimens.

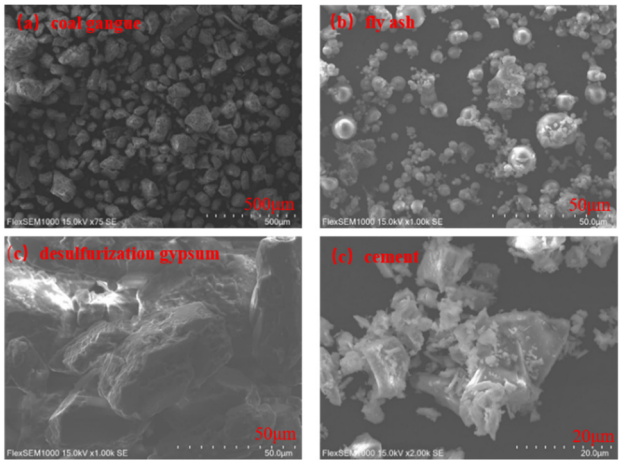


Fig 3. Material SEM analysis

2.2. Experimental Scheme

According to the designed mix proportions, the coal-based solid waste materials were weighed and placed into a container for pre-mixing until a uniform distribution was achieved. Subsequently, mixing water was gradually added, and the materials were thoroughly blended using a handheld electric mixer to produce a homogeneous backfill slurry without noticeable segregation. The slurry was carefully prepared and evenly poured into cubic molds with dimensions of 75 mm × 75 mm × 75 mm. After casting, the specimens, along with the molds, were placed in a high-temperature curing chamber under controlled environmental conditions. The curing temperatures were set at 20 °C, 27.5 °C, 35 °C, 42.5 °C, and 50 °C, while maintaining a relative humidity of 90%. The solidification process was regularly monitored throughout. After 24 hours, the specimens were demolded and returned to the curing chamber for further curing periods at 3, 7, 14, and 28 days. For each curing temperature, six replicate specimens were prepared for each age.

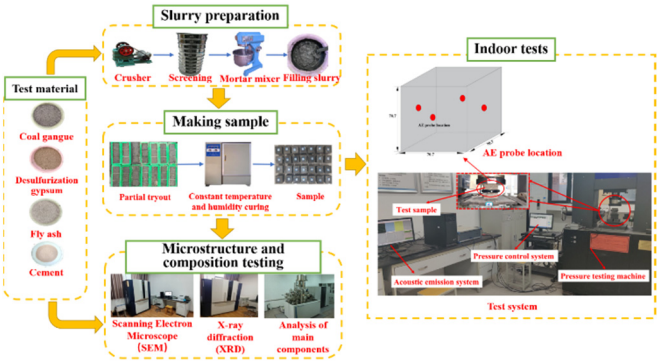


Fig 4. Compression test flow chart

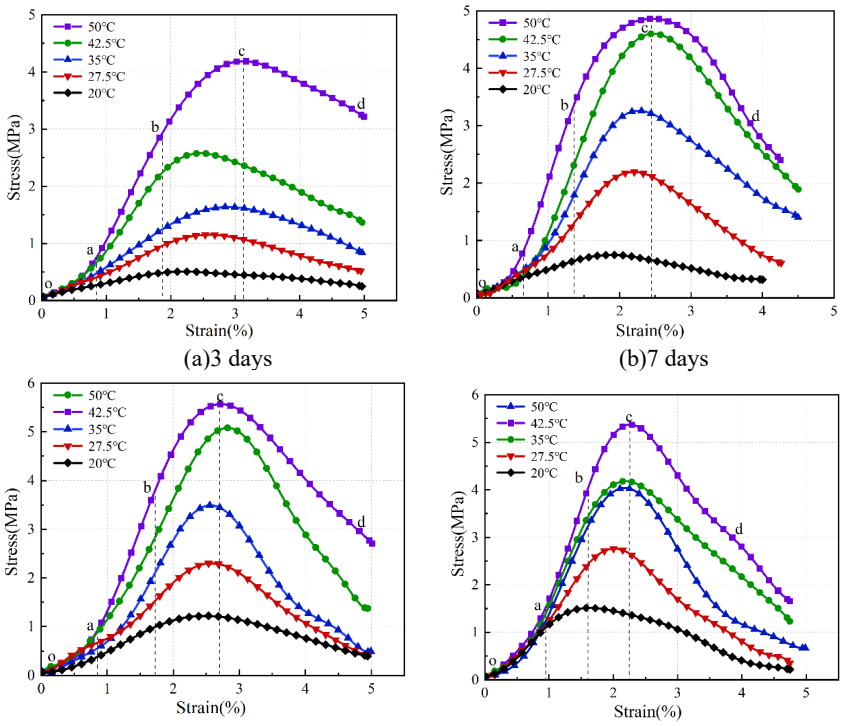
After completion of the curing process, uniaxial compression experiments were performed with a servo-controlled hydraulic rock mechanics system. The tests were implemented under displacement-controlled conditions at a constant loading rate of 0.01 mm/s. Specimen preparation and uniaxial compression procedures were conducted in accordance with the T/GRM 087-2023 Technical

Specification for Laboratory Preparation and Mechanical Testing of Cemented Backfill. Throughout the testing process, axial force, axial displacement, loading duration, as well as the corresponding axial stress and strain were recorded continuously. Meanwhile, the deformation behavior and failure patterns of the specimens were carefully examined. For each testing condition, six parallel specimens were tested, and the mean value was adopted to represent the uniaxial compressive strength of the cemented backfill. The detailed experimental procedure is illustrated in Fig. 4 [21].

3. Results Analysis and Discussions

3.1. Analysis of Stress-strain Curve

Based on the uniaxial compression test results of coal-based solid waste backfill, the stress-strain behavior was analyzed to elucidate the deformation and failure characteristics under uniaxial loading conditions. Fig. 5 compares the stress-strain responses of backfill specimens subjected to uniaxial compression at different curing temperatures and curing ages. The results indicate that variations in curing temperature and age exert no substantial influence on the overall deformation behavior of the specimens. According to the morphological features of the stress-strain curves, the uniaxial compression behavior of the backfill can be divided into four characteristic stages, namely pore compaction (stage oa), linear elastic deformation (stage ab), yielding and damage (stage bc), and post-peak failure (stage cd). As illustrative cases, the deformation and failure processes of specimens cured at 35 °C and 50 °C for 3 d are shown in Fig. 5.



(a)3 days (b)7 days

(c)14 days (d)28 days

Fig 5. Graph of stress versus strain

As shown in Fig. 5, during the initial curing periods (3 d, 7 d, and 14 d), coal-based solid waste backfill specimens subjected to higher temperatures demonstrate a faster increase in axial stress. Consequently, the slope of the stress-strain curve in the linear elastic region, which corresponds to the elastic modulus, rises with increasing curing temperature. Furthermore, both the peak stress before failure and the associated peak strain exhibit a positive correlation with curing temperature. In the post-peak failure phase, the rate of stress reduction in the backfill becomes more pronounced with higher curing temperatures. In addition, both the peak stress prior to failure and the corresponding peak strain show a positive correlation with curing temperature. In the post-peak failure stage, the stress reduction rate of the backfill increases with curing temperature, indicating more pronounced brittle failure behavior or stress softening at higher temperatures. At the later curing stage (28 d), both the peak stress and peak strain reach their maximum values at a curing temperature of 42.5 °C. When the curing temperature is further increased to 50 °C, the descending slope of the post-peak stress-strain curve becomes significantly steeper than that observed at lower temperatures, suggesting that excessively high curing temperatures weaken the load-bearing capacity of coal-based solid waste backfill at later ages.

3.2. Analysis of Energy Evolution Law

3.2.1. Energy Calculation Principle

Under external loading, the backfill initially undergoes elastic deformation, during which elastic strain energy is accumulated. As the applied load increases, internal damage gradually develops, accompanied by energy loss. Consequently, during the loading and failure stages of the backfill, the external work is primarily converted into elastic strain energy and energy dissipation. Under complex stress conditions, according to the first law of thermodynamics [23], and assuming that all the external work is converted into elastic strain energy and dissipated energy, the energy per unit volume of the backfill can be expressed as:

$$U = U_0 + U_1 \quad (1)$$

In the equation: U denotes the total energy absorbed per

unit volume of the specimen (kJ/m³), U_0 represents the dissipated energy (kJ/m³), and U_1 refers to the elastic strain energy (kJ/m³).

The expressions for the total energy and elastic strain energy of the specimen element can be written as follows:

$$U = \int_0^{\varepsilon_0} \sigma_0 d\varepsilon_0 + \int_0^{\varepsilon_1} \sigma_1 d\varepsilon_1 + \int_0^{\varepsilon_2} \sigma_2 d\varepsilon_2 \quad (2)$$

$$U_1 = \frac{1}{2}\sigma_0\varepsilon_3 + \frac{1}{2}\sigma_1\varepsilon_4 + \frac{1}{2}\sigma_2\varepsilon_5 \quad (3)$$

$$\varepsilon_i = \frac{1}{E_i}[\sigma_i - \mu_i(\sigma_j + \sigma_k)](i = 3,4,5) \quad (4)$$

In the equation: σ_0,σ_1,σ_2 denote the maximum, intermediate, and minimum principal stresses, respectively; ε_0,ε_1,ε_2 represent the total strains in the corresponding principal stress directions; ε_3,ε_4,ε_5 are the elastic strains in each principal stress direction; μ_i is Poisson's ratio, and E is the elastic modulus.

Under uniaxial loading, the circumferential stress and deformation are both 0, that is, $\sigma_1 = \sigma_2 = 0$. Combined with the formula, the elastic strain energy can be expressed as:

$$U = \int_0^{\varepsilon_i} \sigma_0 d\varepsilon_0 = \sum_{i=1}^{n} \frac{1}{2}(\sigma_{0(i)} + \sigma_{0(i-1)})(\varepsilon_{0(i)} - \varepsilon_{0(i-1)}) \quad (5)$$

$$U_1 = \frac{1}{2}\sigma_0\varepsilon_0 = \frac{1}{2}\sigma_0\frac{\sigma_0}{E_0} = \frac{\sigma_0^2}{2E_0} \quad (6)$$

3.2.2. Energy Evolution Law

To systematically investigate the energy evolution characteristics of coal-based solid waste backfill under different curing temperatures, specimens cured for 28 d were selected for analysis. The corresponding energy parameters are summarized in Table 1. At a curing duration of 28 d, the elastic strain energy at peak stress exhibits a temperature-dependent trend, with its highest value occurring at 42.5 °C. Beyond this critical temperature, the capacity of the backfill to retain elastic energy at later ages decreases, which manifests macroscopically as a reduction in load-bearing performance.

Table 1. Peak point energy parameters of coal-based solid waste filling body

Ages /day	Maintenance temperature /°C	U_e(kJ/m^3)	U_d(kJ/m^3)	U(kJ/m^3)	U_e/U
28 d	20	17.40	8.71	26.11	66.7%
	27.5	24.60	14.33	38.93	63.2%
	35	28.36	19.46	47.82	59.3%
	42.5	35.92	20.53	56.45	63.7%
	50	25.89	14.70	40.58	63.8%

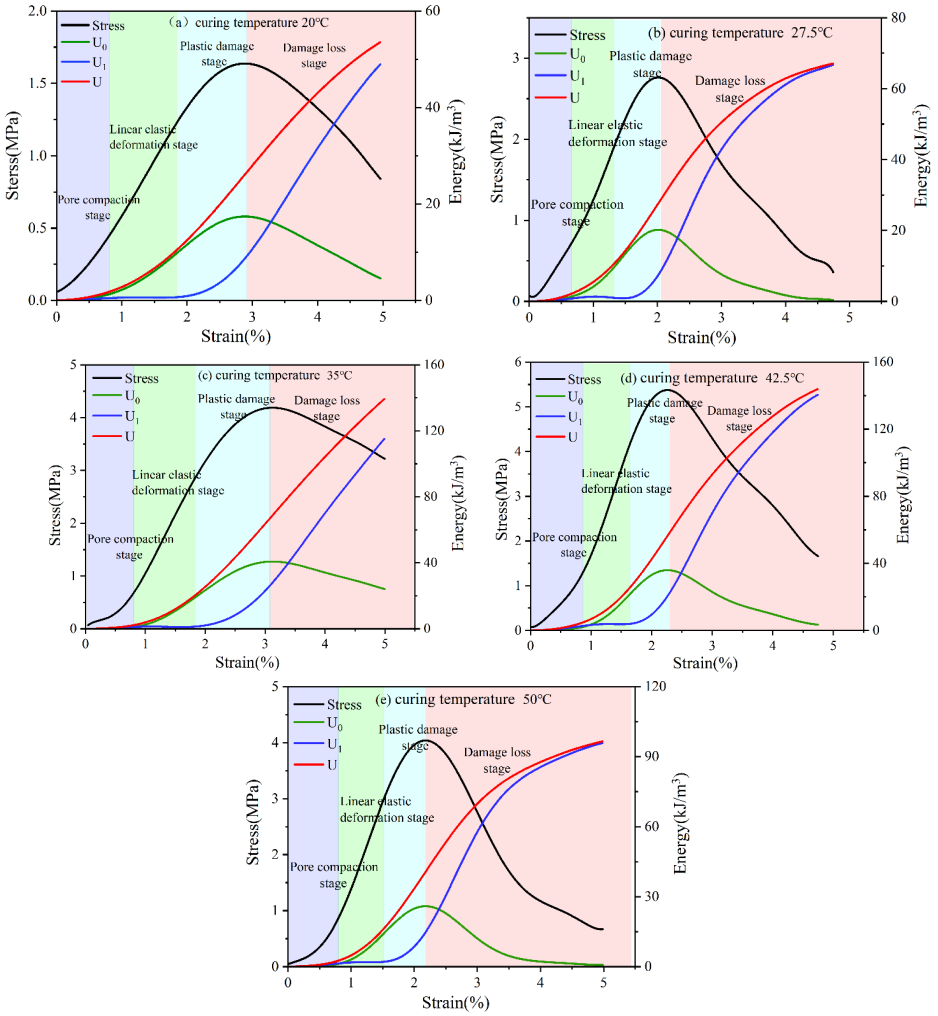


Fig 6. Enegy evolution law

Across different curing temperature conditions, the stress-strain responses of coal-based solid waste backfill specimens display broadly consistent curve profiles, suggesting that changes in curing temperature exert only a minor effect on the intrinsic energy transformation behavior of the backfill. Accordingly, specimens cured for 28 d were selected as representative samples to further examine the energy distribution and evolution during compression-induced failure under varying curing temperatures. Fig. 6 presents the corresponding energy evolution characteristics of coal-based solid waste backfill specimens at a curing age of 28 d for different curing temperatures.

Fig.6 illustrates the evolution of different energy components of coal-based solid waste backfill under uniaxial compression. With increasing strain, the energy components at various deformation stages exhibit evident nonlinear growth characteristics. By examining the strain-dependent evolution of energy parameters under different curing temperatures, the energy distribution and evolution behavior of the specimens can be classified into four characteristic stages.

(1) Pore compaction stage

In this stage, pre-existing pores and microcracks within the specimens are progressively compressed. Due to the relatively low axial stress, the total energy level remains limited. At curing temperatures of 20 °C, 27.5 °C, 35 °C, 42.5 °C, and 50 °C, the proportions of dissipated energy are 35.3%, 42.8%, 50.9%, 58.9%, and 55.7%, respectively. These results demonstrate that energy dissipation dominates the initial compaction stage, and the fraction of dissipated energy generally increases with curing temperature. This behavior indicates that elevated curing temperatures induce more internal defects and microcrack development, thereby enhancing energy dissipation during pore compaction.

(2) Linear elastic deformation stage

During the linear elastic deformation stage, the specimens continue to absorb external energy, which is mainly accumulated in the form of elastic strain energy, whereas the dissipated energy remains nearly unchanged. For curing temperatures of 20 °C, 27.5 °C, 35 °C, 42.5 °C, and 50 °C, the proportions of elastic strain energy reach 92.7%, 92.7%, 90.8%, 88.5%, and 82.9%, respectively. As curing temperature increases, the contribution of elastic strain energy shows an overall declining trend, suggesting that higher curing temperatures accelerate damage evolution during the elastic stage and facilitate earlier energy dissipation.

(3) Plastic damage stage

In this stage, the growth rate of elastic strain energy decreases, while dissipated energy gradually increases; however, elastic strain energy remains the dominant component. When the curing temperatures are 20 °C, 27.5 °C, 35 °C, 42.5 °C, and 50 °C, the elastic strain energy proportions are 66.5%, 64.1%, 58.9%, 62.8%, and 63.4%, respectively. Overall, the influence of curing temperature on energy distribution in this stage is relatively limited.

(4) Damage lossstage

Following peak stress, the release of elastic strain energy accelerates, accompanied by a pronounced increase in dissipated energy. When the accumulated elastic energy surpasses the energy-bearing capacity of the material, macroscopic crack propagation is rapidly activated, resulting in an abrupt conversion of stored energy into dissipation. This intensified damage evolution ultimately leads to a substantial degradation of the load-bearing capacity of the backfill.

4. Conclusion

Based on uniaxial compression experiments and energy evolution analyses of coal-based solid waste backfill cured under various temperatures and ages, the mechanical behavior and failure characteristics of the backfill were systematically examined. The principal findings can be summarized as follows:

(1) Curing temperature exerts a strong age-dependent effect on the mechanical performance of coal-based solid waste backfill. At early curing stages (3-14 d), elevating the curing temperature markedly increases the elastic modulus, peak stress, and peak strain as a result of accelerated hydration processes. At a curing age of 28 d, both strength and deformation capacity exhibit a non-monotonic response to curing temperature, attaining optimal values at 42.5 °C. Further temperature elevation to 50 °C intensifies post-peak softening and reduces load-bearing capacity, demonstrating that excessively high curing temperatures impair the long-term mechanical performance of the backfill.

(2) Under uniaxial compression, the stress-strain response of coal-based solid waste backfill displays stable stage characteristics. Independent of curing temperature, the stress-strain curves maintain similar overall profiles and can be consistently categorized into four stages: pore compaction, linear elastic deformation, yielding damage, and post-peak failure. These results suggest that curing temperature primarily influences energy distribution and damage severity at each deformation stage, rather than fundamentally altering the deformation mode.

(3) Curing temperature plays a critical role in regulating the energy storage and dissipation behavior of the backfill. At a curing age of 28 d, both elastic strain energy and total energy at peak stress show a non-monotonic dependence on curing temperature, reaching maximum values of 35.92 kJ/m³ and 56.45 kJ/m³, respectively, at 42.5 °C. When the curing temperature is increased to 50 °C, elastic strain energy decreases significantly, indicating a reduced capacity for energy storage and a consequent decline in load-bearing performance at later ages.

(4)Elevated curing temperatures promote early damage development and alter the energy evolution path.With increasing curing temperature, the proportion of dissipated energy during the pore compaction stage increases from 37.5% to 59.3%, while the proportion of elastic strain energy during the linear elastic stage decreases continuously. This demonstrates that high-temperature curing introduces more initial damage and microcracks, causing a greater portion of external work to be dissipated prematurely and leading to enhanced brittleness during subsequent failure.

Acknowledgments

The Project was supported by the National Natural Science Foundation of China (No.52404106).

References

[1] Qian Minggao, Xu Jialin. Coal mining and strata movement [J]. Coal Journal, 2019, 44 (04) : 973-98

[2] Zhang Jixiong, Zhang Qiang, Zhou Nan, et al. Research progress and prospect of coal-based solid waste filling mining technology [J]. Coal Journal, 2022, 47 (12) : 4167-4181.

[3] Yang KH, Mun JS, Jeong J E. Compressive Strength Development of High-Strength Concrete under Different Curing Temperatures[J]. Advanced Materials Research, 2014, 905(195-8).

[4] Kim JK, Moon YH, Eo SH. Compressive strength development of concrete with different curing time and temperature[J]. Cement and Concrete Research, 1998, 28(12): 1761-1773.

[5] Su Hongyan, Song Pingxin, He Qiang. Mechanical properties and energy evolution of cemented tailings backfill under different curing temperatures [J]. Journal of Mining and Strata Control Engineering, 2023, 5 (02) : 55-65.

[6] Li Zhi, Guo Qinqiang, Yang Yong, et al. Study on macro-meso multi-scale temperature-strength coupling characteristics of backfill [J]. Gold, 2023, 44 (12) : 5-9 + 13.

[7] Chen Qiusong, Zhang Qi, et al.. Temperature variation of strength and leaching toxicity of phosphogypsum backfill [J]. Chinese Journal of Nonferrous Metals, 2021, 31 (04) : 1084-1095.

[8] Zhang Peng, Zhang Wensheng, Wei Jiangxiong, et al. The effect of curing temperature on the strength and hydration products of red mud-slag alkali-activated cementitious materials [J]. New building materials, 2017, 44 (10) : 1-3 + 1.

[9] Liu Weizhen, Guo Zhongping, Huang Wanpeng, et al. Experimental study on triaxial unloading pressure characteristics of cemented backfill after curing at different temperatures [J]. Journal of Rock Mechanics and Engineering, 2022, 41 (11) : 2268-2282.

[10] Bai Liwei, Zhao Runkang, Qu Chunlai, et al. Experimental study on the effect of curing temperature on the mechanical properties of cemented backfill [J].Gold, 2021,42 (11) : 33-38.

[11] Jiang Feifei, Zhou Hui, ShangJia, et al. Effects of temperature and age on the physical and mechanical properties of gravel sand cemented backfill [J]. Journal of Central South University, 2020, 27 (10) : 2999-3012.

[12] Fall M, Celestin J C, Pokharel M. A contribution to understanding the effects of curing temperature on the properties of mine cemented tailings backfill[J]. Engineering Geology, 2010, 114: 397-400.

[13] Wu D, Cai S. Coupled effect of cement hydration and temperature on hydraulic behavior of cemented tailings backfill[J]. Journal of Central South University, 2015, 22(5): 1956-1964.

[14] Xu Wenbin, Wan Changbing, Tian Xichun. Coupling effect of temperature fissure on strength of backfill and crack propagation mode [J]. Journal of Mining and Safety Engineering, 2018,35 (03) : 612-619.

[15] Liu Chao, Han Bin, Sun Wei, et al. Experimental study and industrial application of strength characteristics of waste rock broken cemented backfill in alpine region [J]. Journal of Rock Mechanics and Engineering, 2015, 34 (01) : 139-147.

[16] H Jiang, M Fall, L Cui. Freezing behaviour of cemented paste backfill material in column experiments[J]. Construction and Building Materials, 2017, 147: 837-846.

[17] Cui Lizhuang. Study on strength and creep characteristics of unclassified tailings cemented backfill at different curing temperatures [D]. Qingdao: Qingdao University of Science and Technology, 2021.

[18] Yang Xiaoliang. Study on failure characteristics of backfill and backfill-surrounding rock cementation surface under different curing temperatures [D].Wuhan : Wuhan University of Science and Technology, 2021.

[19] Liu W, Chen J, Guo Z, et al. Mechanical properties and damage evolution of cemented coal gangue-fly ash backfill under uniaxial compression: Effects of different curing temperatures [J]. Construction and Building Materials, 2021, 305: 124820.

[20] Duan Yun, Wang Qicai, Yang Zijiang, et al.. Study on the thermal damage effect of steam curing on high strength machine-made sand concrete [J]. Journal of Lanzhou Jiaotong University, 2022,41 (05) : 6-12

[21] Zhang Jiqiang, Yang Ke, Xiang H, et al. Study on mechanical properties and damage characteristics of coal-based solid waste cemented backfill [J]. Construction and Building Materials, 2023, 368.

[22] Solecki R, Conant R J. Advanced Mechanics of Materials[M]. London: Oxford University Press, 2003.

[23] Wen Zhiqiang. Experimental study on mechanical properties of coal-based solid waste backfill under different curing temperatures [D]. Anhui University of Science and Technology, 2024. DOI : 10.26918 / d.cnki.ghngc.2024.000382.